PERGAMON

Journal of Structural Geology 24 (2002) 827–846

JOURNAL OF STRUCTURAL GEOLOGY

www.elsevier.com/locate/jstrugeo

Three-dimensional geometry of large-scale fault-propagation folds in the Cantabrian Zone, NW Iberian Peninsula

Mayte Bulnes*, Jesús Aller

Departamento de Geología, Facultad de Geología, Universidad de Oviedo, 33005 Oviedo, Spain

Received 3 August 2000; revised 15 March 2001; accepted 5 June 2001

Abstract

In the western part of the Cantabrian Zone, a transition occurs from a southern zone mainly dominated by thrusts to a northern zone where folds predominate. Detailed structural analysis within the 'transitional' zone reveals that large-scale fault-propagation folds constitute the structural framework of this area. The topography, together with variations in plunge of the fold axes, allows us to visualize their three-dimensional geometry. They exhibit a complex internal structure due to thrusting before, during, and after major folding. Thrusts are the structures that accommodate most of the shortening in deep levels, whereas the shortening is accommodated stratigraphically upward by major fault-propagation folds, imbricate thrust systems and minor structures. In general, during the initial stages of fold amplification, the backlimb of the antiforms thickened, whereas during the latter stages their forelimbs thinned. After folding, the major folds were translated and rotated due to emplacement of younger thrusts located in the foreland. Although these natural large-scale fault-propagation folds are more complex than many theoretical models proposed up to date, certain specific structural features observed in the field examples can be explained by comparing them with theoretical models.

Keywords: Transitional zone; Large-scale fault-propagation folds; Thrusts

1. Introduction

The Cantabrian Zone is the external portion of the Variscan Cordillera in the northwestern part of the Iberian Peninsula and consists of a foreland fold-thrust belt that involves a pre- and a syn-orogenic sequence of Paleozoic age. The structures within the Cantabrian Zone describe an eastward-concave arc (Asturian Arc). In the study area, located in the western part of the Cantabrian Zone (Sobia and Aramo units), thrusts and folds comprise the main structures of the arc (Fig. 1). In this area and zones farther N, folds predominate, whereas to the S, out of the study area, thrusts are the most conspicuous structures (Fig. 1). This apparent variation in structural style along the strike of the main structures was documented in previous studies (e.g. Soler, 1967; Pello, 1972; Julivert and Arboleya, 1984; Alonso et al., 1991; Alonso and Marcos, 1992).

As a general rule, thrusts and folds are closely related in the Cantabrian Zone. Therefore, investigating the manner and significance in which the coexistence between folds and thrusts takes place are crucial to understand the change in structural style from S to N. In this sense, the main aim of this paper is to identify the geometrical features of folds and thrusts, as well as to establish their structural evolution, variations along strike, and relative timing. To achieve this objective, we have used a 1:20,000 geological map presented by Bulnes (1995, 1999), and seven cross-sections parallel to the tectonic transport direction, based on Bulnes (1995), that allow us to visualize the deformation styles and their evolution in the vertical and lateral directions. Our three main objectives are to: (1) supply new data to understand the relationships between Variscan folds and thrusts in the western units of the Cantabrian Zone, (2) provide new insights into thrust/fold development in foreland thrust-fold belts, and (3) show new three-dimensional geometrical and kinematic patterns of fault-related folds.

2. Thrusts and folds geometry

2.1. Structural outline

At first sight, the structural framework of the study area consists of a large number of folds and thrusts developed at different scales. However, a careful inspection of the geological map and cross-sections (Figs. 2–9) reveals that the folds can be grouped from W to E into a fold train formed by

* Corresponding author. Tel.: +34-985-103116; fax: +34-985-103103.
E-mail address: maite@asturias.geol.uniovi.es (M. Bulnes).

0191-8141/02/$ - see front matter
PII: S0191-8141(01)00114-6

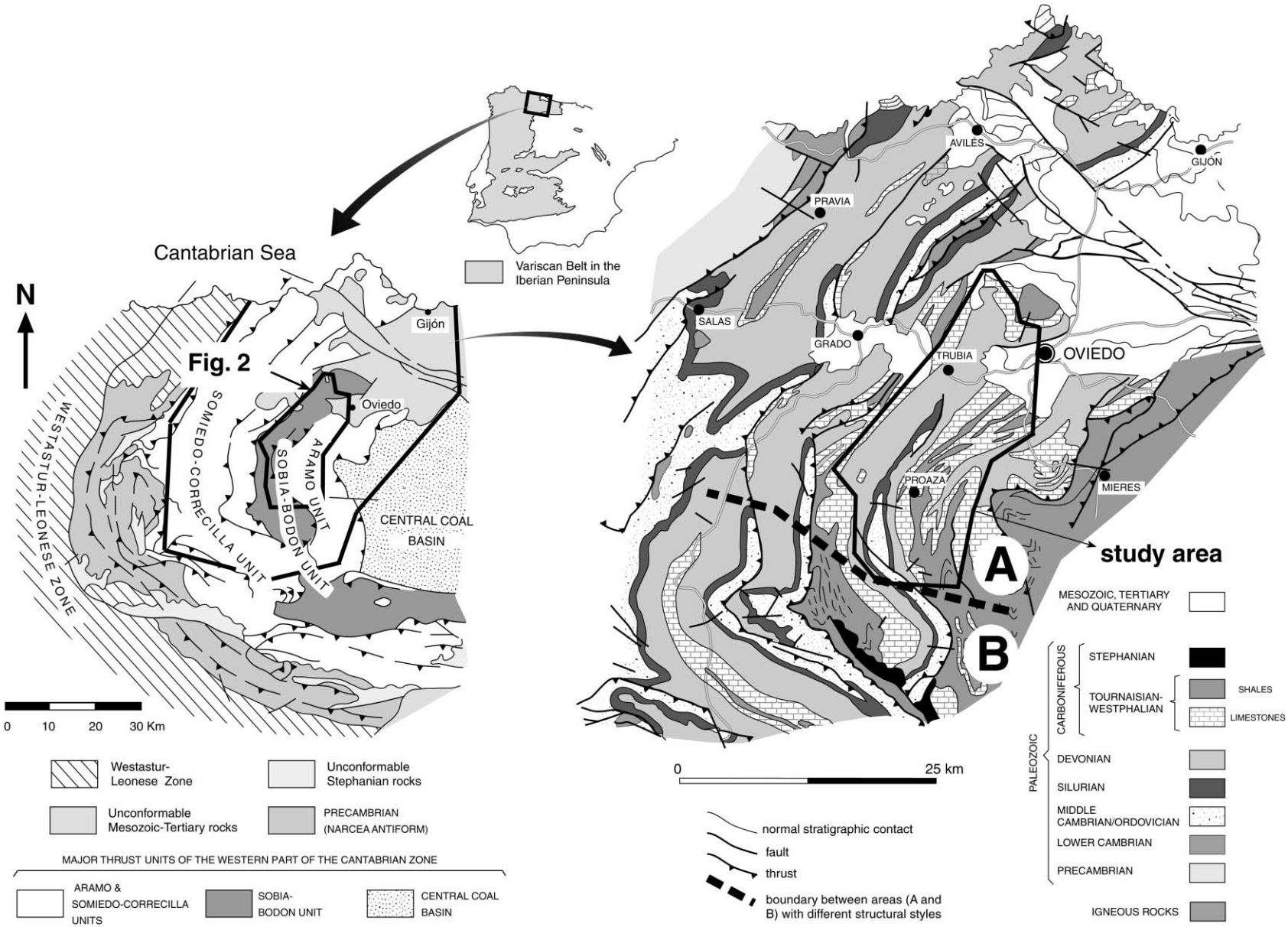

Fig. 1. Structural sketch of the western part of the Cantabrian Zone (modified after Pérez-Estaún et al., 1988). The thick dashed line across the Somiedo–Correcilla, Sobia–Bodón and Aramo units separates areas with different structural styles. Thrusts are the most important structures to the S (region B), whereas folds predominate to the N (region A).

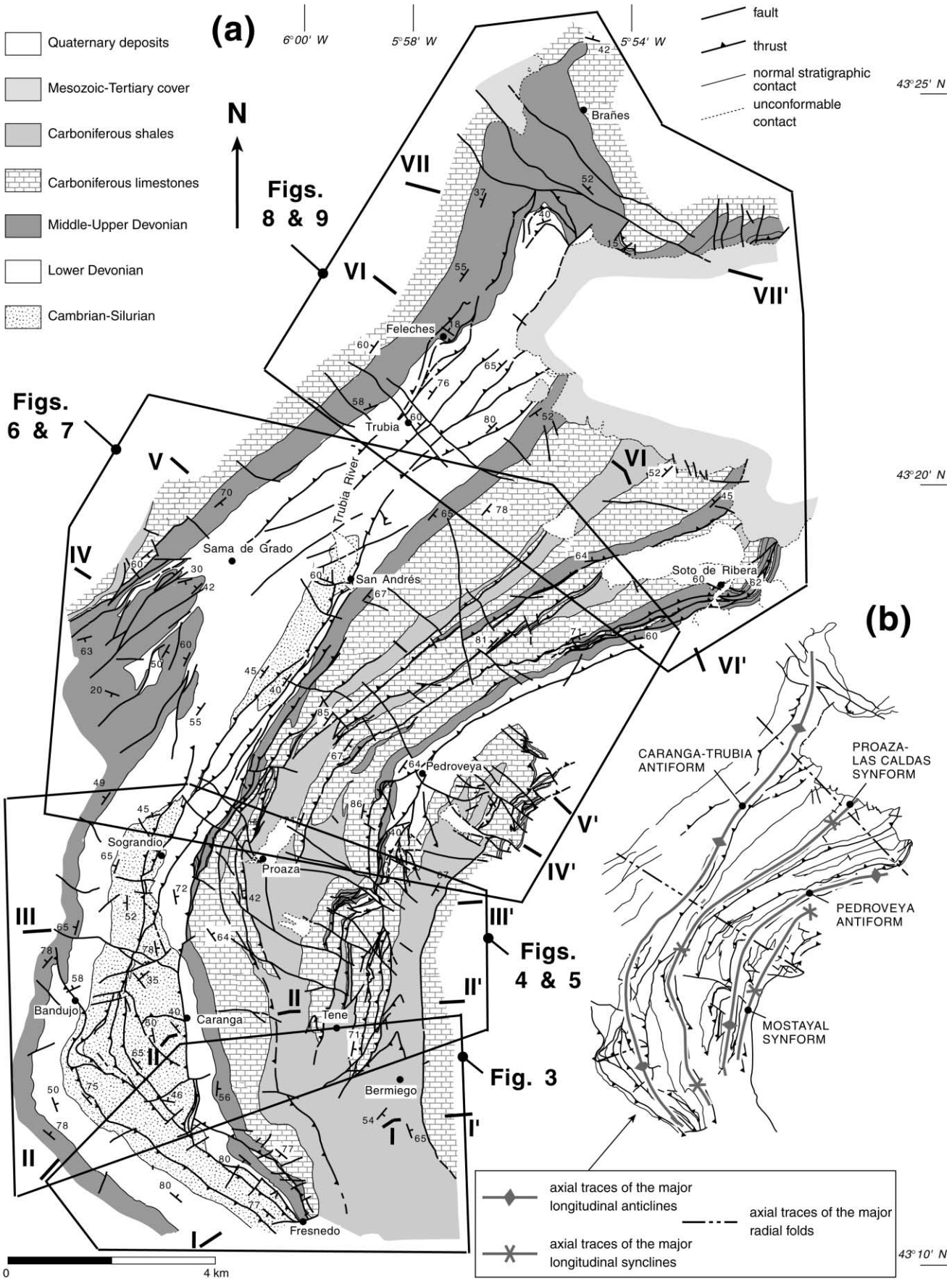

Fig. 2. (a) Geological map and (b) structural sketch of the study area that shows the major folds (modified after Bulnes, 1995).

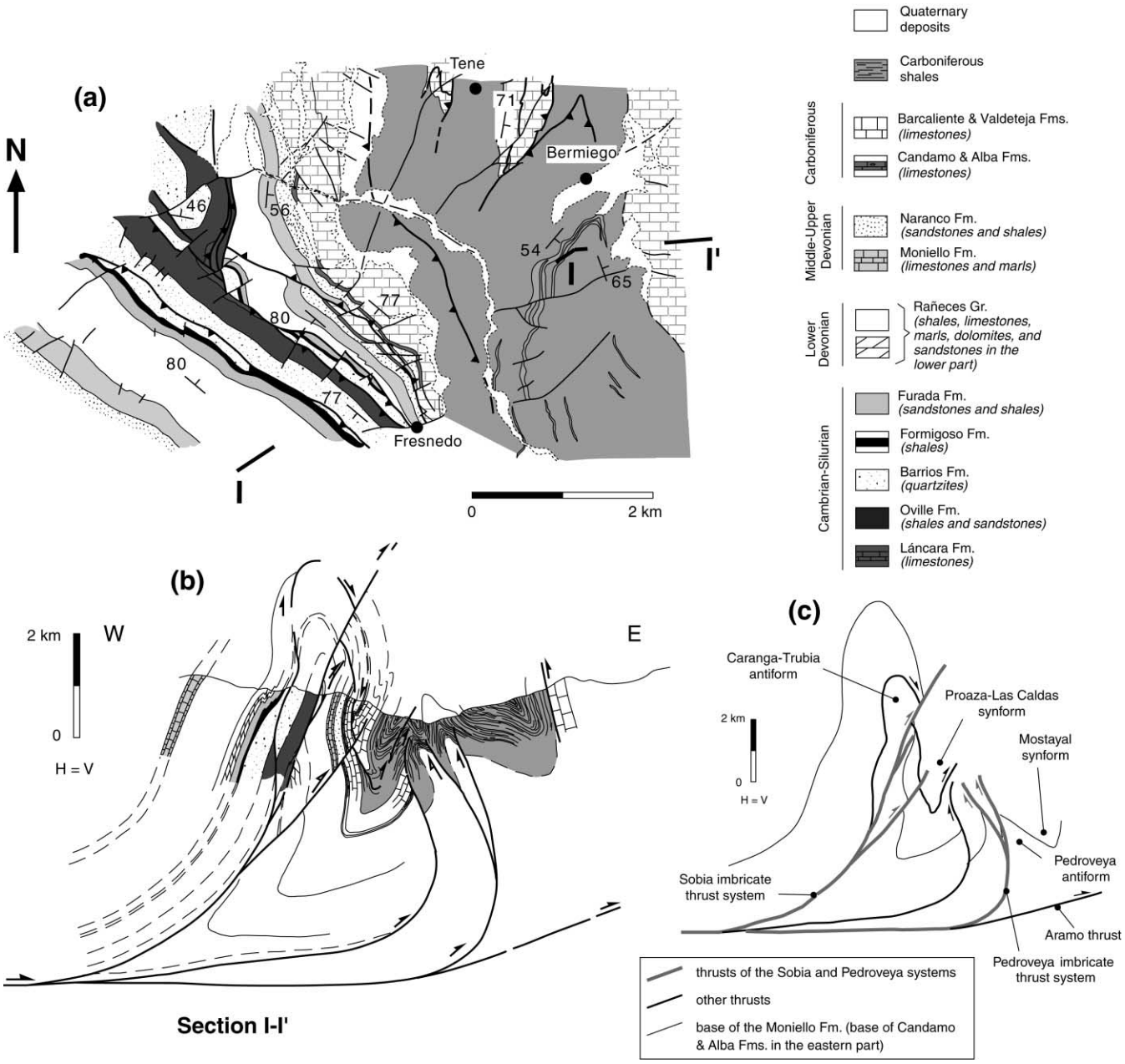

Fig. 3. (a) Detailed geological map of the southern part of the study area, (b) cross-section I–I′ and (c) simplified sketch of cross-section I–I′ through this area.

two major antiforms and synforms: the Caranga–Trubia antiform, the Proaza–Las Caldas synform, the Pedroveya antiform and the Mostayal synform. They are kilometer-scale folds, with the westernmost being the largest (Figs. 2–9). These major folds trend NE–SW in the northern part of the study area, N–S in the central part, and NW–SE in the southern part. Their traces follow the geometry of the Asturian Arc (Figs. 1 and 2). Map-scale folds perpendicular to them appear in some localities (Fig. 2b).

The large-scale folds exhibit a complex internal structure resulting from the emplacement of thrusts before, during, and after folding (Bulnes, 1995). Examples of folded thrusts, which are also cut and offset by younger thrusts, can be found in the southern part of the study area near the Caranga and Tene villages (Figs. 2–5), and in the northern part of the study area between the Trubia and Brañes villages (Figs. 2a, 8 and 9). The map traces of the thrusts formed during or after folding are approximately parallel or slightly oblique to those of the major folds described above (Fig. 2). These thrusts have been grouped into two imbricate thrust systems: the Sobia imbricate thrust system in the western half of the study area, and the Pedroveya thrust system in the eastern half (Figs. 2–9). According to Bulnes (1995) and Bulnes and Marcos (2001), the tectonic transport vectors point towards the core of the Asturian Arc (i.e. towards the ENE in the southern part of the study area, towards the E

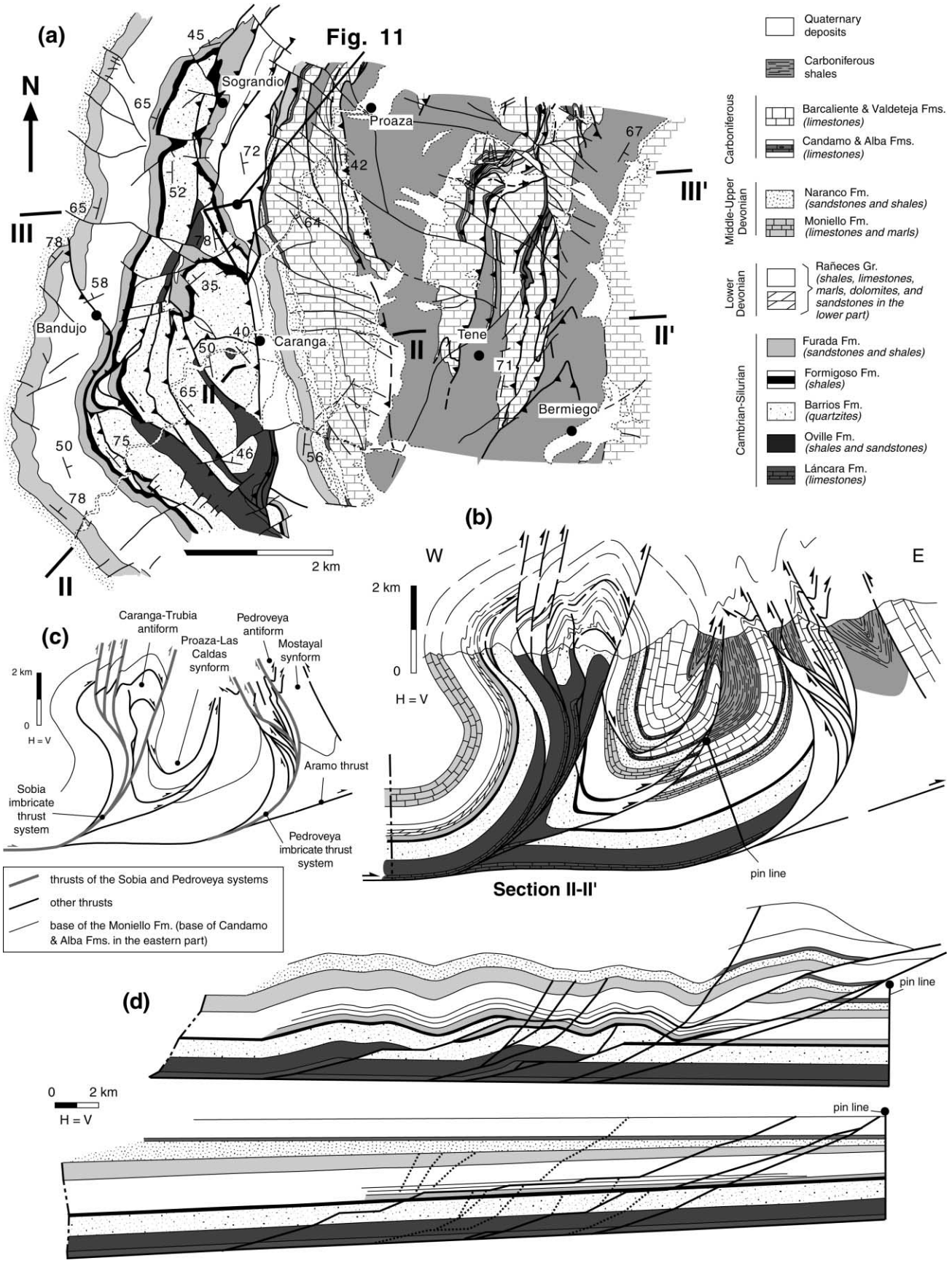

Fig. 4. (a) Detailed geological map of the area between Sograndio and Bermiego villages, (b) cross-section II–II′, (c) simplified sketch of cross-section II–II′ through this area, and (d) partial and total restorations of cross-section II–II′. The limestone pattern of the Valdeteja, Barcaliente and Moniello Formations has been omitted for clarity in the restored sections. The scale of the present-day section is twice the scale of the restored sections.

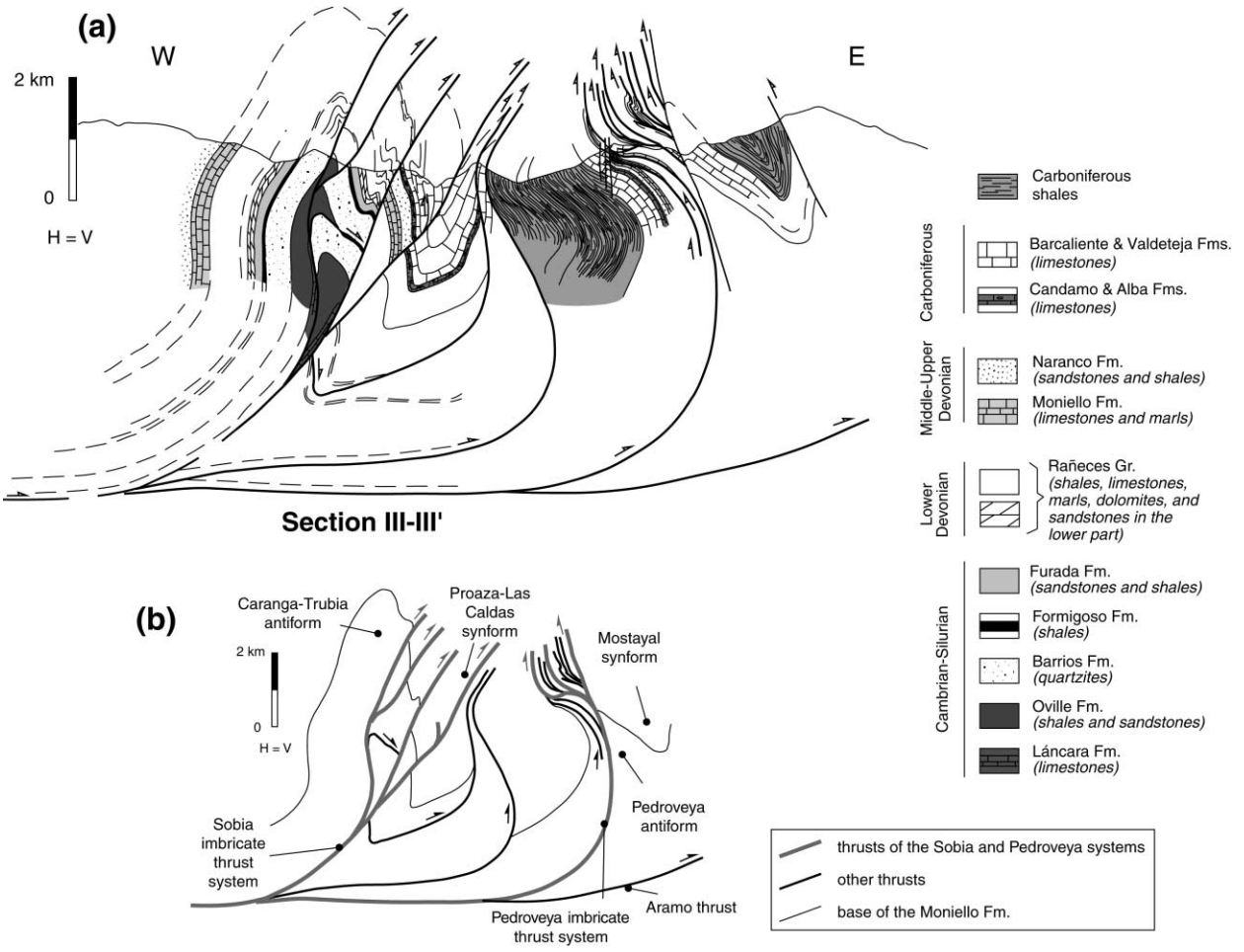

Fig. 5. (a) Cross-section III–III′ and (b) simplified sketch of cross-section III–III′. See geological map in Fig. 4a for location of the cross-section.

in the central part, and towards the SE in the northern part). A number of late faults that involve dip or oblique/slip displacements oriented oblique/transverse with respect to the main structures also appear in the study area.

Folds and thrusts deform a thick Cambrian to Carboniferous sequence that consists of alternations of shales, sandstones and limestones with sporadic thick units formed by dolomites/limestones, quartzites and shales. The Variscan age of the structures is well established. With the exception of a few steeply-dipping faults with dominant NW–SE strikes, the rest of the structures are sealed by the Mesozoic deposits that unconformably overlie the Paleozoic succession in the northern part of the study area (Fig. 2).

Different stratigraphic units crop out along the strike of the major longitudinal structures due to the plunge of the fold axes, which ranges from horizontal to moderate towards both N and S (Fig. 10). The distribution of the different stratigraphic units along strike is also influenced to a lesser extent by some late faults. In general, the rocks that crop out within the Caranga–Trubia antiform are progressively younger towards the N, whereas within the Pedroveya antiform they are progressively younger towards the S.

2.2. Thrust/fold structural relationships

At regional scale, the lateral transition from thrusts (to the S) into folds (to the N) (Fig. 1) suggests that these two types of structures may be genetically related. For instance, we have observed some fault-bend folds caused by the staircase geometry of the oldest deformed thrusts (e.g. gentle flexures of the beds in the westernmost part of the cross-sections in Figs. 3–5 due to the occurrence of hanging wall and/or footwall ramps). Nevertheless, the large-scale folds mentioned previously are not related to the oldest deformed thrusts, but to other imbricate thrust systems discussed below.

Seven sections across the study area illustrate the geometry of the thrusts and folds (Figs. 3–9). The structure at depth has been constructed using regional data, section-balancing techniques, the geological interpretations of a regional-scale seismic profile (Pérez-Estáun et al., 1994, 1995; Gallastegui et al., 1997), and the excess-area method (Chamberlin, 1910) to calculate the detachment depth in cross-sections involving folds (for more details see Bulnes and Marcos (2001)). It has been assumed that the thrusts merge into a 4–5 km depth detachment located at the base

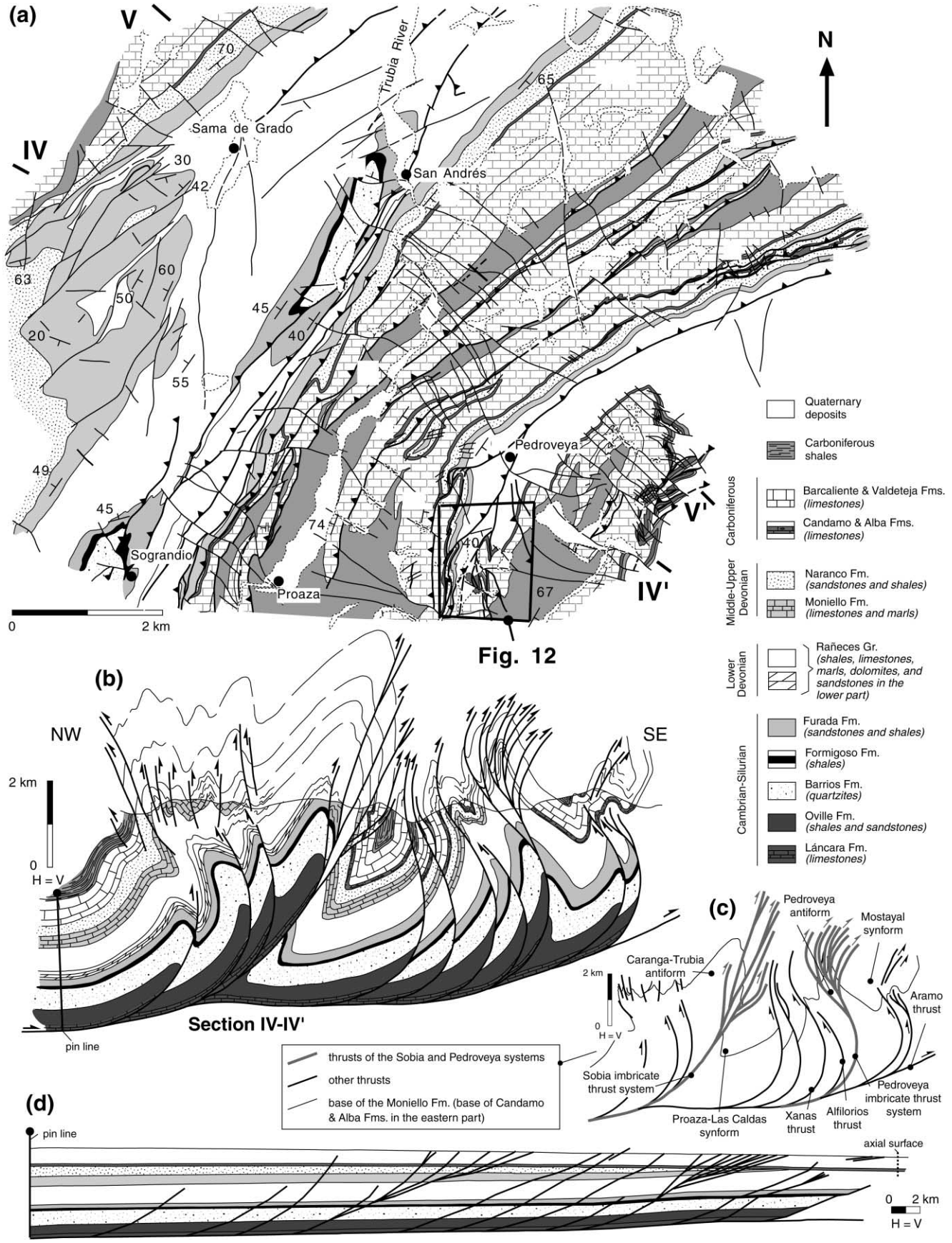

Fig. 6. (a) Detailed geological map of the area around Sama de Grado, Sograndio and Pedroveya villages, (b) cross-section IV–IV′, (c) simplified sketch of cross-section IV–IV′ through this area, and (d) restoration of cross-section IV–IV′. The limestone pattern of the Valdeteja, Barcaliente and Moniello Formations has been omitted for clarity in the restored sections. The scale of the present-day section is three times the scale of the restored sections.

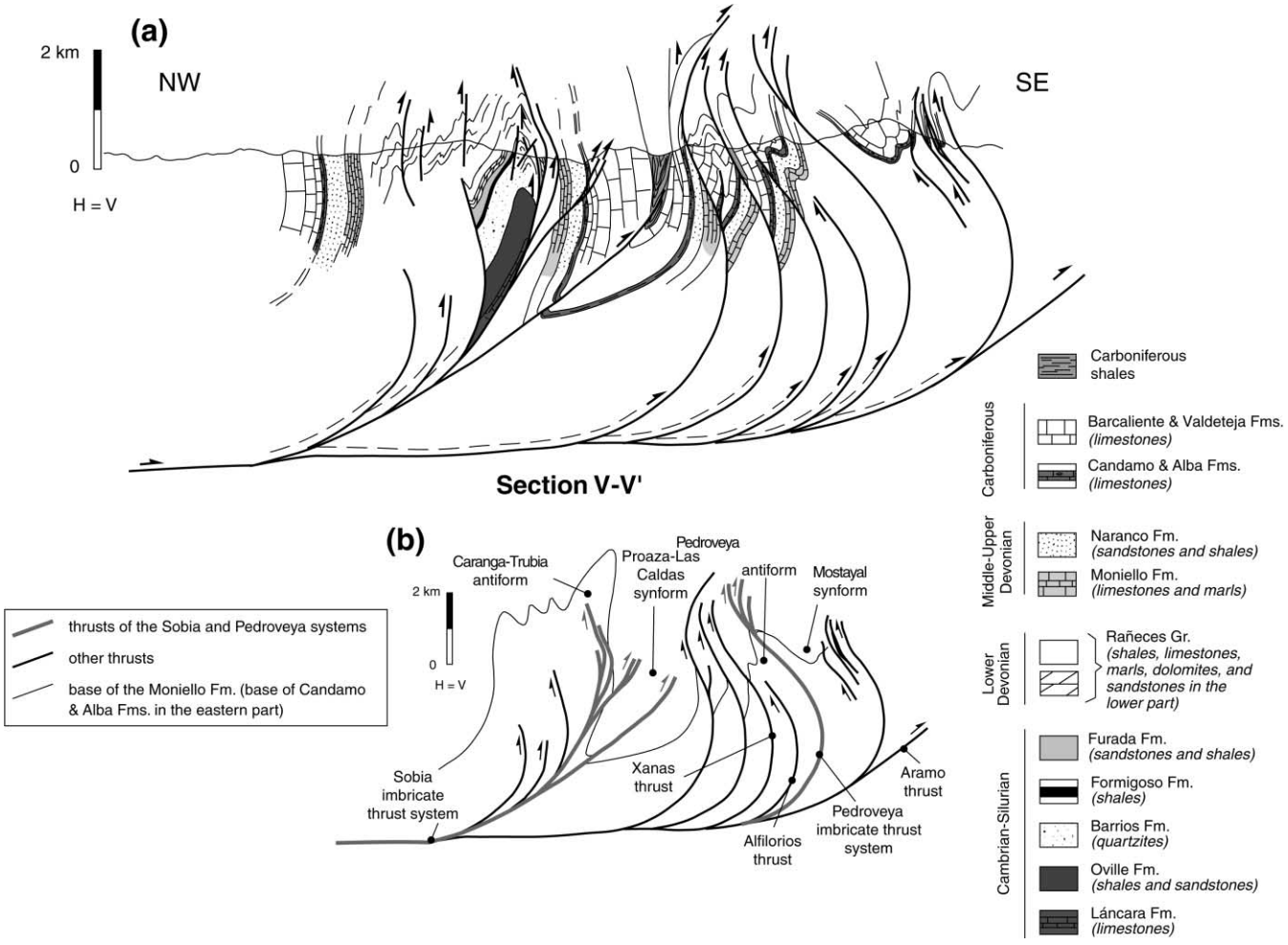

Fig. 7. (a) Cross-section V–V′ and (b) simplified sketch of cross-section V–V′. See geological map in Fig. 6a for location of the cross-section.

of the Láncara Formation (Lower Cambrian) because it is the oldest stratigraphic unit that crops out in the study area and adjacent regions, and because this stratigraphic horizon is a well-known regional detachment level in the Cantabrian Zone. The depth to detachment, estimated by carrying the surface geology to depth maintaining the dips and thicknesses of the stratigraphic packages measured in the field (Figs. 4b and 6b), is in accordance with the geological interpretations of the regional-scale seismic profile ESCIN-1 that extends across the central part of the study area from W to E (Pérez-Estáun et al., 1994, 1995; Gallastegui et al., 1997). In addition, Bulnes and Marcos (2001) applied the Chamberlin (1910) method to several sections across the study area and concluded that the basal detachment should be located between 4 and 5 km depth. Bulnes and Marcos (2001) proposed an alternative interpretation for the sections across the study area in which the eastern thrusts may merge into a detachment located within the Silurian or Devonian sequences. This alternative is used to explain the absence of Cambrian to Silurian rocks and the smaller size of the folds in the eastern half of the study area. The occurrence of a shallower detachment in the eastern part does not modify significantly the timing and kinematic evolution of the structures described in this study.

Due to the complex internal structure of the major folds, a simplified map and cross-sections have been constructed to better visualize the main features (Figs. 2–9). In addition, two restored sections (Figs. 4d and 6d) and one partial restoration (Fig. 4d) were constructed to test the viability of the cross-sections and to compare the degree of deformation before and after the emplacement of the imbricate thrust systems. The equal line-length and equal-area methods have been used to restore the cross-sections. The geometrical features illustrated in the simplified map and sketches, and in the restored sections helped us to determine the structural relationships between the large-scale folds and the imbricate thrust systems.

The partial restoration of the western part of cross-section II–II′ (Fig. 4d) reveals that the two major folds located to the W are mainly related to the propagation of the Sobia imbricate thrust system. Assuming a similar evolution to the E, the major folds in the E are mainly related to the emplacement of the Pedroveya imbricate thrust system. The simplified structural sketches show that: (1) the folds

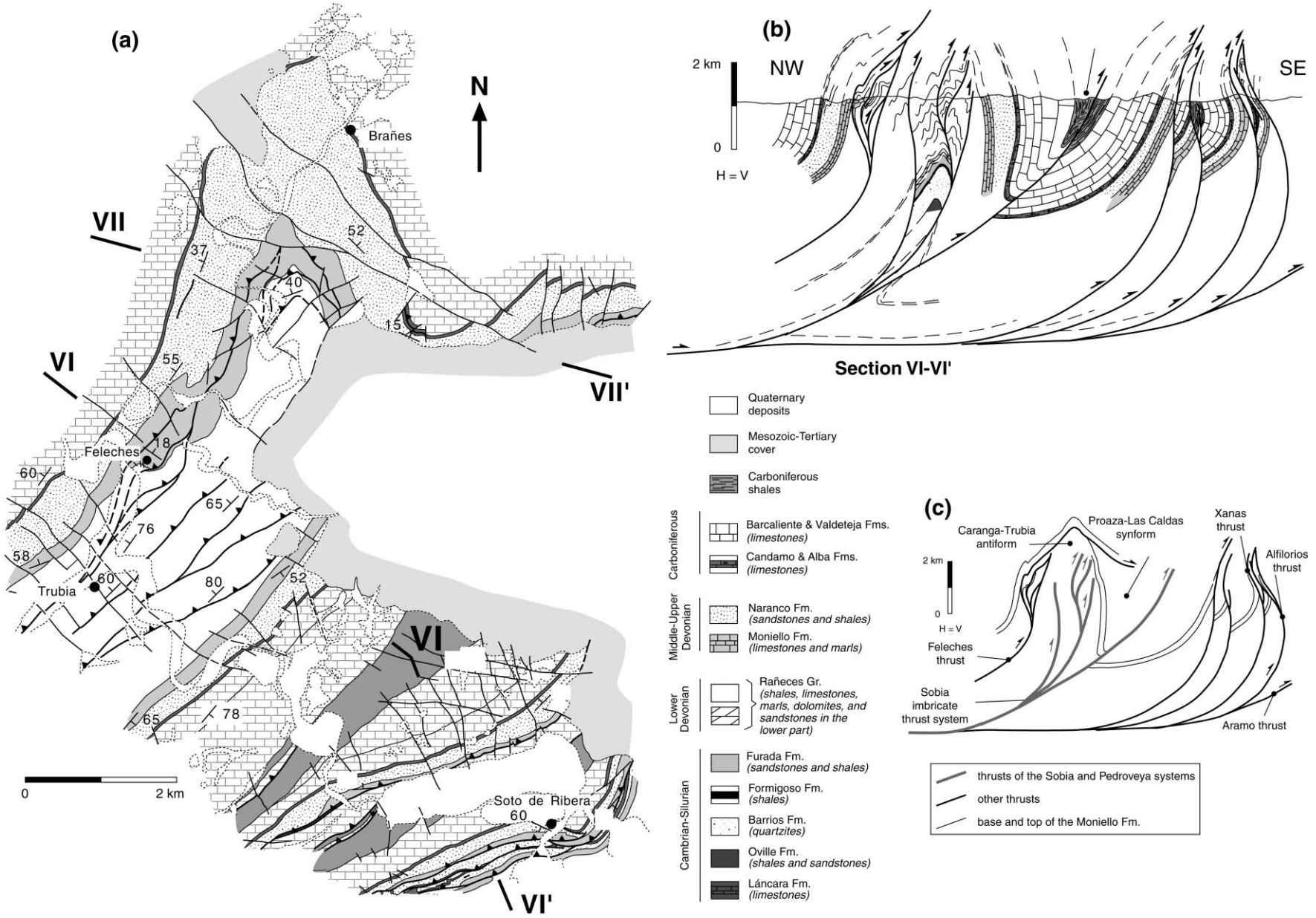

Fig. 8. (a) Detailed geological map of the area around Trubia, Brañes and Soto de Ribera villages, (b) cross-section VI–VI′, and (c) simplified sketch of cross-section VI–VI′ through this area.

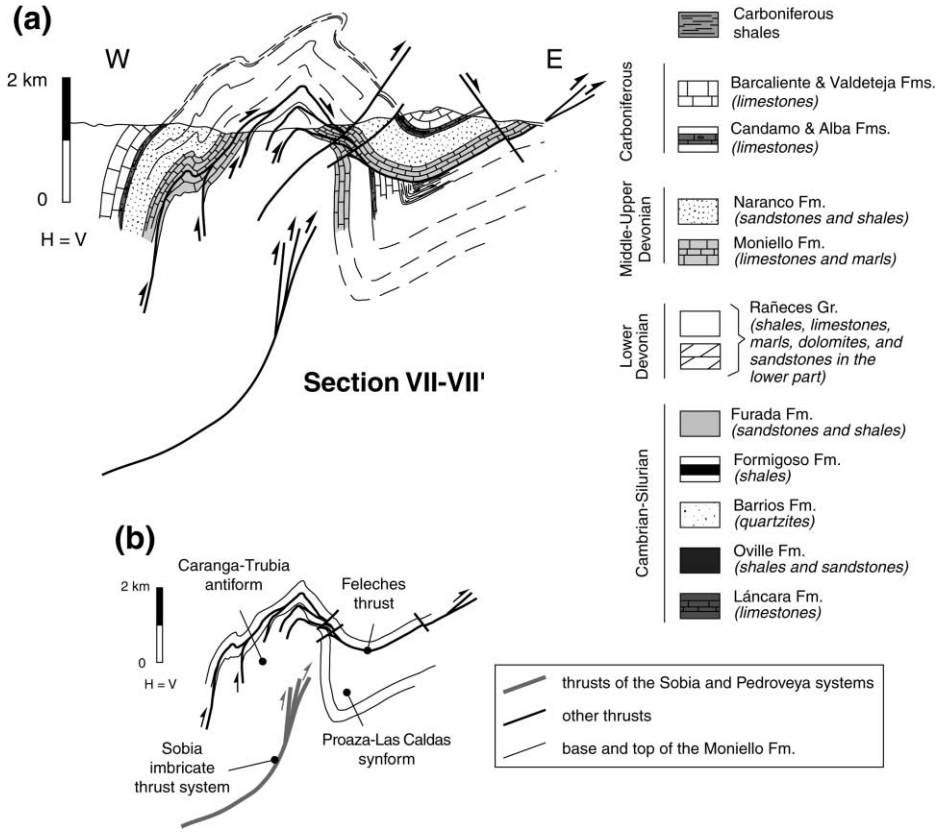

Fig. 9. (a) Cross-section VII–VII′ and (b) simplified sketch of cross-section VII–VII′. See geological map in Fig. 8a for location of the cross-section.

are asymmetric, (2) they are tight structures with small interlimb angles, (3) the spatial distribution of the folds is closely related to the position of the thrust systems, (4) the strike of the folds and thrusts is approximately parallel, (5) for each fold pair, the antiform overlies most of the imbricate thrusts, whereas the synform underlies most of them, (6) the backlimbs of the antiforms are long and their average dip is similar to the dip of the thrusts (except for those cases in which the limbs are distorted by other structures), (7) the forelimbs of the antiforms are shorter and show numerous imbricate thrusts, (8) the dimensions of the folds and thrusts are similar, and (9) the sum of displacement along the imbricate thrusts decreases up-section. These observations also suggest that the large-scale folds and the imbricate thrust systems are genetically related. In particular, many of the geometrical features and structural relationships between them agree with those observed in fault-propagation folds (Suppe, 1985; Jamison, 1987). According to this, the Caranga–Trubia antiform and the Proaza–Las Caldas synform are a fold pair associated with the Sobia imbricate system, whereas the Pedroveya antiform and the Mostayal synform are a fold pair related to the Pedroveya imbricate system (Bulnes, 1995, 1999).

Apart from the map-scale folds, there is a large number of fault-bend, fault-propagation and detachment folds at outcrop scale. For instance, some detachment folds crop out to the N of the Caranga village (Fig. 11). To the NW of the Pedroveya village, a large number of fault-bend and fault-propagation folds develop within the Carboniferous rocks.

2.3. Three-dimensional thrust/fold geometry

Variations in the plunge of the major fold axes and in the displacement along the transverse faults allow us to visualize the geometrical evolution of the structures as they involve progressively younger Paleozoic rocks. The fold plunge is due to thrust sheet stacking, which led to rotation and deformation of the folds, fold terminations and local interference with radial folds (Bulnes, 1995). Therefore, analyzing several cross-sections parallel to the tectonic transport directions can unravel the three-dimensional geometry of the structures and help to understand their kinematic evolution. To better understand the three-dimensional geometry of the major structures, the Sobia imbricate thrust system and its related folds (Caranga–Trubia antiform and Proaza–Las Caldas synform) will be described separately from the Pedroveya imbricate thrust system and its related folds (Pedroveya antiform and Mostayal synform).

2.3.1. Lateral and vertical evolution of the Sobia imbricate thrust system, the Caranga–Trubia antiform, and the Proaza–Las Caldas synform

To the S of the study area, the Sobia thrust is a

Fig. 10. Structural sketch of the study area showing the orientation of the fold axes.

well-exposed structure that places Cambrian rocks over Carboniferous rocks (e.g. García Fuente, 1952, 1959; Marcos, 1968; Marcos et al., 1980; Fig. 1). Nevertheless, within the study area, it evolves into an imbricate thrust system and a pair of major fault-propagation folds (Bulnes, 1995, 1999).

The geological map (Fig. 2a) shows that, in general, the core of the Caranga–Trubia antiform is occupied by progressively younger rocks to the N. Two fold culminations are responsible for the variations in the plunge of the fold axis. One of the culminations is located between Fresnedo and Sograndio villages (Figs. 2–5). In this area, the steep dip of the structures combined with the erosion led to the formation of a tectonic window, which allows deep thrust sheets to crop out. This culmination may have been produced by the superposition of numerous thrust sheets that disappear laterally (Bulnes and Marcos, 2001). A smaller fold culmination near the San Andrés village allows pre-Silurian rocks to crop out in this area (Figs. 2a and 6a). From this fold culmination to the N, there is a large outcrop of Lower Devonian rocks due to the subhorizontal disposition of the fold axes (Figs. 2a, 6a and 8a), and in the northernmost sector the Devonian and Carboniferous rocks exhibit a periclinal termination caused by a moderate N plunge of the fold axes (Figs. 2a and 8a).

The Caranga–Trubia antiform and the Proaza–Las

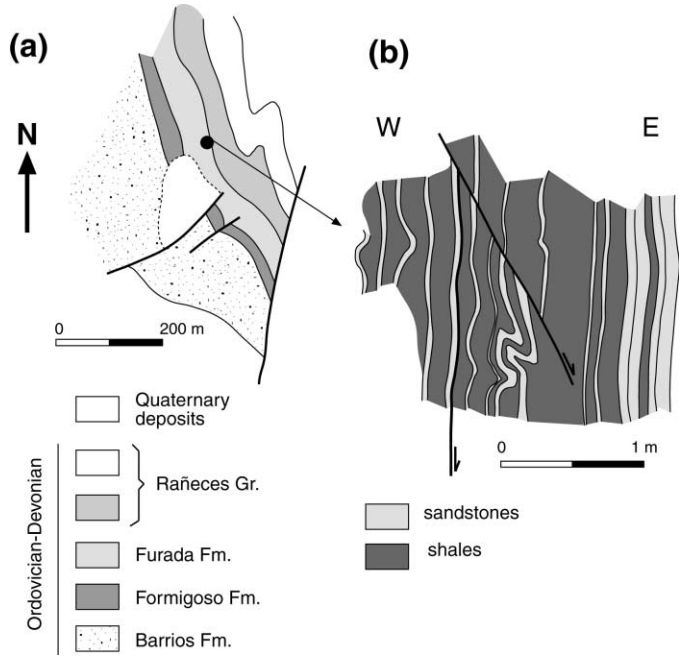

Fig. 11. Outcrop-scale detachment folds developed within the Silurian rocks. (a) Geological map and (b) field cross-section. See geological map in Fig. 4a for location.

Caldas synform exhibit a complex internal structure due to thrusting before, during, and after folding (Figs. 3–9). Thus, the geometry of these folds is strongly controlled by variations in the number of thrusts along strike, their geometry, and the amount of displacement. In general, the axial surfaces of the Caranga–Trubia antiform and the Proaza–Las Caldas synform dip steeply towards the W, the backlimb of the antiform and the eastern limb of the

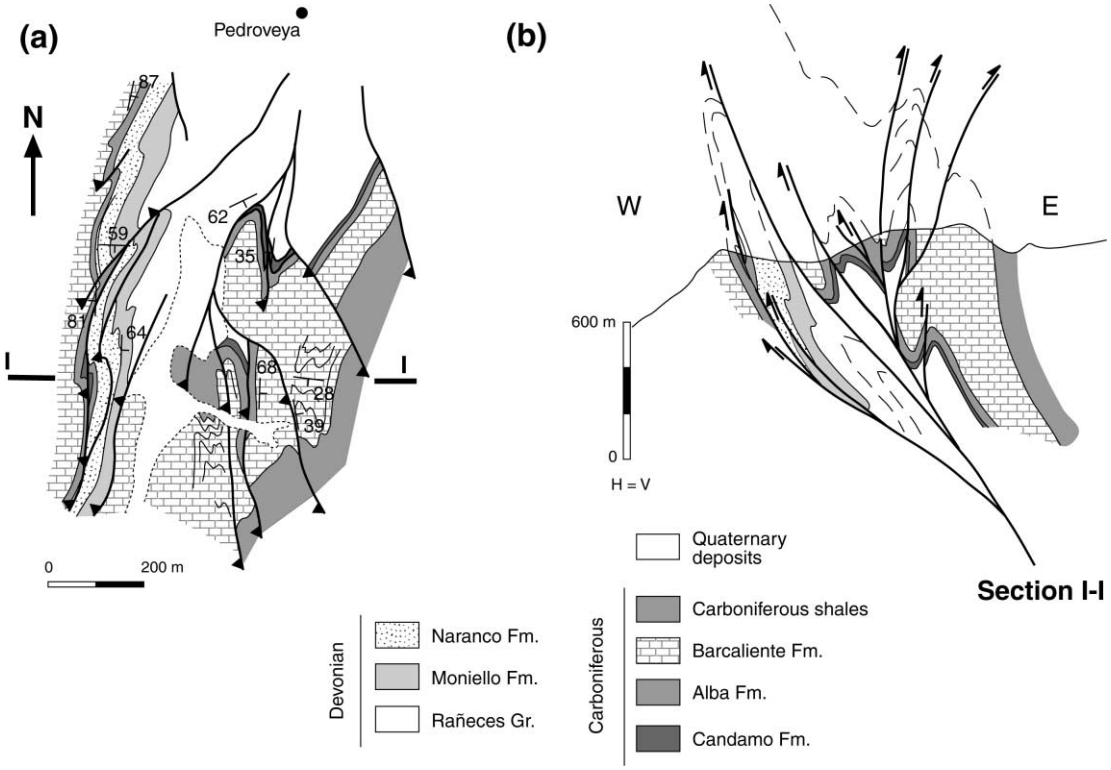

Fig. 12. (a) Detailed geological map of the area to the S of the Pedroveya village and (b) cross-section through this area. See geological map in Fig. 6a for location.

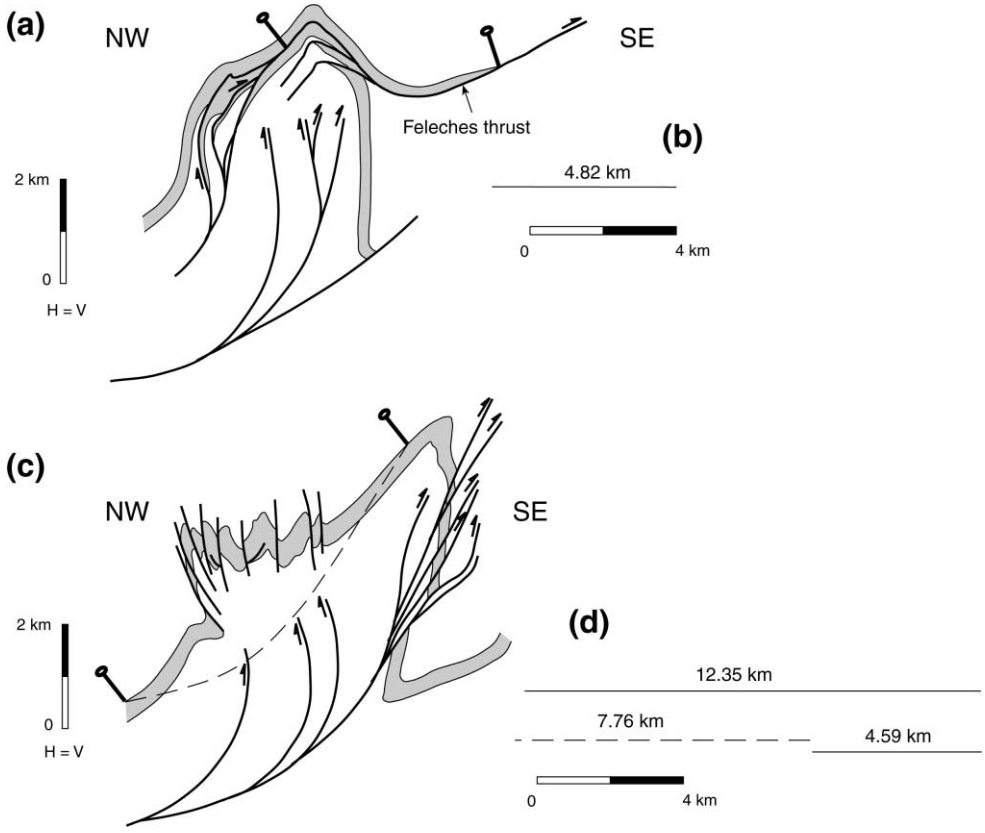

Fig. 13. (a) Detailed geometry of the Feleches thrust in the western part of cross-section VI–VI′ in Fig. 8. (b) Minimum displacement along the Feleches thrust estimated using the top of the Lower–Middle Devonian limestones as a reference surface in the cross-section illustrated in (a). (c) Detailed cross-section showing the folds developed in the western part of cross-section IV–IV′ in Fig. 6 and possible geometry of the Lower–Middle Devonian limestones assuming no folds (dashed line). (d) Comparison between the length of the westernmost part of the cross-section illustrated in (c) (7.76 km) and the top of the Lower–Middle Devonian limestones once the effect of folds and faults has been removed (located between the pin lines; 12.35 km).

synform dip between 50 and 80° to the W, and the common limb of both folds is subvertical or dips steeply to the E.

The general geometry described above varies along strike. The most significant variations involve the dip of the backlimb of the Caranga–Trubia antiform. In the southern part of the study area, the backlimb dips are steep to the W (upper part of the backlimb in cross-section II–II′ in Fig. 4) to moderate to the E (lower part of the backlimb in cross-section II–II′ in Fig. 4). This dip variation is due to thrusts that cut the backlimb and the hinge of the antiform, and cause rotation of the thrust sheets during progressive thrust emplacement, and explains the increased rotation toward the W. Cross-section IV–IV′ shows a 'protuberance' developed in the backlimb of the Caranga–Trubia antiform (Fig. 6) that has been attributed to thrusts at depth (Bulnes, 1989, 1995). In some localities, the axial surface of the Caranga–Trubia antiform dips steeply to the E, whereas elsewhere it dips to the W. The disposition of the axial surface mainly depends on the amount of translation of the antiform along the main thrust(s) of the Sobia imbricate thrust system and on the local dip of this listric thrust(s). For instance, the axial surface in the pre-Silurian rocks dips to the W in cross-section VI–VI′ (Fig. 8), and to the E in cross-section II–II′ (Fig. 4).

Regarding the Proaza–Las Caldas synform, Carboniferous rocks occupy its core all along the study area, and its geometric variations along strike are small. In some areas, the Proaza–Las Caldas synform resembles a box fold (e.g. cross-section IV–IV′ and V–V′ in Figs. 6 and 7, respectively). This shape is interpreted to result from bed rotation induced by development of the Pedroveya antiform and the Mostayal synform located to the E and their translation over a thrust surface that dips 20–30° degrees to the W.

The Caranga–Trubia antiform and the Proaza–Las Caldas synform have an atypical geometry due to older thrusting. The older thrusts can be observed in the southern part of the study area (cross-sections I–I′, II–II′, and III–III′ in Figs. 3–5, respectively; Bulnes, 1991, 1992, 1995, 1999) and in the northern part (cross-sections VI–VI′ and VII–VII′ in Figs. 8 and 9, respectively; Bulnes, 1995, 1999). In the southern part of the study area, the older thrust surfaces are tightly folded by the Caranga–Trubia antiform and the Proaza–Las Caldas synform, and largely offset by the Sobia imbricate thrust system (Figs. 3–5), whereas they are less folded and offset in the northern part. The older thrusts caused a large number of bed obliquities and thickness changes before major folding (see partial restored section of cross-section II–II′ in Fig. 4).

The branch lines mapped in the study area support the interpretation that a large number of thrusts belonging to the Sobia imbricate thrust system merge into a single thrust (Figs. 2–9). In the southern part of the study area, the Sobia thrust system consists of several imbricates that repeat the pre-Silurian succession, and cut the limbs and hinge of the Caranga–Trubia antiform (cross-sections I–I′, II–II′ and III–III′ in Figs. 3–5, respectively). Nevertheless, to the N closely spaced splays appear, mainly in the forelimb of the Caranga–Trubia antiform and in the hinge of the Proaza–Las Caldas synform, both occupied by Devonian and Carboniferous rocks (cross-sections IV–IV′, V–V′ and VI–VI′ in Figs. 6–8, respectively). The influence of these thrusts on the geometry of the major folds depends on their location within the folds. The imbricate thrusts that offset the backlimb and hinge of the antiform produce repetitions of the stratigraphic succession (beds dip less than the thrust surfaces), whereas the thrusts that offset the forelimb of the antiform cause the absence of part of the stratigraphic succession (beds dip more than the thrust surfaces). This results in thickening of the backlimb of the Caranga–Trubia antiform and thinning of its forelimb.

2.3.2. Lateral and vertical evolution of the Pedroveya imbricate thrust system, the Pedroveya antiform, and the Mostayal synform

To the SW of the Soto de Rivera village, a thrust that duplicates the Lower Devonian rocks has been mapped by Bulnes (1995) (Fig. 2a). To the S around the Pedroveya village, this thrust evolves into the Pedroveya imbricate thrust system and a pair of major fault-propagation folds (Bulnes, 1995, 1999; Fig. 6).

The three-dimensional geometry of the Pedroveya antiform and the Mostayal synform will be described using cross-sections I–I′ to V–V′ (Figs. 3–7, respectively), as only the westernmost part of the antiform appears in cross-section VI–VI′ (Fig. 8). Only Devonian and Carboniferous rocks crop out within these two major folds, and their cores are occupied by progressively younger rocks southwards. The disposition of rocks at the surface, together with the periclinal termination of the antiform to the S and the periclinal termination of the synform to the N, indicates an average S plunge of the fold axes (Fig. 2a).

There are some similarities between the fault-propagation folds described in the previous section and the Pedroveya antiform and Mostayal synform. These two folds also exhibit a complex internal structure due to thrusts previous to major folding (cross-sections II–II′ and III–III′ in Figs. 4 and 5, respectively) and thrusts that cut the major folds. In general, the axial surfaces of both folds dip from moderately to steeply to the E, and both folds have small interlimb angles. The E-dipping disposition of the axial surfaces results from the passive rotation due to the emplacement of frontal thrusts. In particular, a rotation of 20–30° could be the consequence of the translation of the major folds in the easternmost part over a W-dipping basal-thrust surface. There are significant variations along strike in the dip of the backlimb of the antiform (from subhorizontal to subvertical; Figs. 5 and 7), and in the dip of the eastern limb of the synform. Similarly to the fault-propagation folds described in the previous section, these dip changes depend on the number and geometry of the thrusts located within the folds.

A major WNW–ESE transverse fault that runs across the Proaza village (Fig. 2a) cuts the Pedroveya antiform and elevates the southern fault block. This fault separates two areas with a slightly different structural configuration. Thrusts previous to major folding have been only identified in the southern fault block (cross-sections II–II′ and III–III′ in Figs. 4 and 5, respectively). In the northern fault block around the Pedroveya village, the Pedroveya imbricate thrust system is comprised of a large number of splays (Figs. 2, 6 and 13). These splays appear in both limbs and in the hinge of the Pedroveya antiform, and involve small displacements. To the S of the fault, only three thrusts within the Pedroveya imbricate thrust system have been mapped: two within the backlimb of the antiform and another one within its forelimb, close to the hinge zone (cross-sections I–I′, II–II′, and III–III′ in Figs. 3–5, respectively). These three thrusts involve greater displacements than the thrusts located in the northern fault block, particularly the one located to the W of the Tene village (Fig. 2a and cross-section II–II′ in Fig. 4). Similarly to the major folds described in the previous section, the thrusts within the Pedroveya antiform backlimb duplicate part of the Paleozoic succession, whereas thrusts within the Pedroveya antiform forelimb omit part of the stratigraphic succession.

In the northern part of the study area, a few thrusts that do not belong to the Pedroveya imbricate thrust system developed in the backlimb of the Pedroveya antiform (Fig. 2a, and cross-sections IV–IV′, V–V′ and VI–VI′ in Figs. 6–8, respectively). The thrust surfaces, and the beds within the thrust sheets, dip moderately to steeply to the E at the topographic surface. This is interpreted as a result of their passive rotation during the subsequent formation of the Pedroveya imbricate thrust system and related folds, and their translation over a W-dipping thrust surface. Therefore, these thrusts predate the formation of the Pedroveya imbricate thrust system and related folds.

3. Shortening accommodation

Bulnes (1995) and Bulnes and Marcos (2001) estimated the amount of shortening by comparing the present-day length of six sections across the study area with the total length of the top of the Moniello Formation (or the base of the Candamo Formation when the Moniello and Naranco Formations are absent). This particular stratigraphic horizon is one of the best represented horizons in all the cross-sections, and it is the top of a competent stratigraphic unit unlikely to have undergone bed-length variations during

deformation. These authors assumed that this stratigraphic horizon was horizontal before deformation. The minimum shortening obtained ranges between 56.9 and 59.4%. In addition, the shortening obtained by comparing the length of the top of the Moniello Formation in the western half of cross-section II–II′ between the pin lines and its restored length (Fig. 4d) is about 60.1%. The shortening obtained in cross-section IV–IV′ between the western pin line and the easternmost axial surface is about 56.8%. Thus, from the values obtained by Bulnes (1995), Bulnes and Marcos (2001), and the new values presented here, it seems that the percentage of shortening is approximately constant irrespective of the along-strike variations in structural style.

3.1. Major thrust/fold systems

In this region, the structures that accommodate the largest amount of shortening are the imbricate thrust systems and the major fault-propagation folds. The two restorations of the western half of cross-section II–II′ (Fig.4d) point out that the Sobia imbricate thrust system and the two related folds (Caranga–Trubia antiform and Proaza–Las Caldas synform) accommodate about 70% of the total shortening in the western part of that section.

Because the Caranga–Trubia and Proaza–Las Caldas fold pair is larger than the Pedroveya and Mostayal fold pair, the structure of the western half of the study area likely involves more shortening. This agrees with the fact that the maximum shortening has been obtained considering only the restoration of the western half of cross-section II–II′ (see previous section).

The main point that supports the interpretation of fault-propagation folds is that the imbricate thrust systems loose displacement and the folds become better developed as they affect progressively younger stratigraphic units. In the next sections we describe the evolution of thrusts into folds and the structures that accommodate shortening from the deepest levels to the highest ones.

3.1.1. The Sobia system

No data are available on the deformation experienced by the lowest part of the Paleozoic stratigraphic sequence within the study area. However, S of the study area, the Lower Cambrian limestones display a large hanging wall flat over the thrust surface. Within the Middle Cambrian succession, the Sobia thrust starts to lose displacement upwards and a pair of folds develops at the thrust tip. This type of structure has been illustrated at deep levels only in cross-sections II–II′ and IV–IV′ (Figs. 4 and 6, respectively).

Major structures that accommodate shortening in the upper part of the stratigraphic sequence are:

(a) two fault-propagation folds: the Caranga–Trubia antiform and the Proaza–Las Caldas synform, and
(b) thrusts of the Sobia imbricate thrust system. In general, these structures accommodate small amounts of shortening in the upper stratigraphic levels. In some cases, the imbricate thrusts do not breakthrough the whole Paleozoic succession, but die in Lower Devonian incompetent units causing map- and outcrop-scale folds (see the thrust tip points in Fig. 2a).

Minor structures that accommodate shortening in the upper part of the stratigraphic sequence include folds related to the imbricate thrusts. Some of the breakthrough imbricate thrusts simply transported beds and older structures, and involved minor distortion. However, some thrusts exhibit associated ramp folds, which distorted the major folds and caused local thickening of their forelimbs. Cross-sections I–I′, III–III′ and IV–IV′ (Figs. 3, 5 and 6, respectively) illustrate some of these map-scale folds developed in the forelimb of the Caranga–Trubia antiform. There are also buckle folds at different scales mainly developed in the incompetent stratigraphic units located in the hinge of the major antiform (e.g. map-scale and many outcrop-scale folds developed within the Lower Devonian rocks in the hinge zone in cross-sections IV–IV′, V–V′ and VI–VI′ in Figs. 6–8, respectively).

Minor faults are pervasive in the study area, and microstructures such as stylolites, developed mainly in the lowest part of the Lower Devonian succession, also help accommodate the deformation.

3.1.2. The Pedroveya system

In the study area and surrounding areas, the Pedroveya system involves only Devonian to Carboniferous rocks (Fig. 2a). However, to construct the cross-sections in Figs. 3–9, we have assumed that the deep structure is similar to that of the Sobia system; i.e. a thrust located at the base of the Lower Cambrian limestones loses displacement within the Middle Cambrian succession and has a pair of fault-propagation folds developed at its tip. Major structures that accommodate shortening upwards include:

(a) two fault-propagation folds (the Pedroveya antiform and the Mostayal synform) which accommodate most of the shortening within this system, and
(b) thrusts of the Pedroveya imbricate thrust system. These thrusts die within the Carboniferous shales (see the thrust tip points in Fig. 2a), where a large number of small-scale folds occur, particularly near the thrust tips.

Regarding minor structures, there are more map- and outcrop-scale folds related to the imbricate thrusts of the Pedroveya system than to thrusts of the Sobia system. For instance, to the S of the Pedroveya village, a large number of fault-propagation folds are related to imbricate thrusts that cut both limbs and the hinge of the Pedroveya antiform (Fig. 12). Minor faults mainly related to the minor folds mentioned above also occur.

3.2. Other map-scale thrust/fold systems

Some of the thrusts developed in the common limb of the Proaza–Las Caldas synform and the Pedroveya antiform evolve laterally and/or vertically into folds (Figs. 6–8). Most of the displacement due to thrusting is accommodated upwards and/or laterally by fault-propagation folding.

The Feleches thrust is one of the earliest thrusts because it developed before the Sobia system and was deformed by the Caranga–Trubia antiform and the Proaza–Las Caldas synform. This thrust runs mainly along the base of the Lower–Middle Devonian limestones (Fig. 2a and cross-sections VI–VI′ and VII–VII′ in Figs. 8 and 9, respectively). The Feleches thrust disappears to the S and a number of well-developed folds and subvertical faults deform the Lower–Middle Devonian limestones (Fig. 2a and cross-section IV–IV′ in Fig. 6). To determine if the Feleches thrust transitions into folds southwards, we have attempted to quantify the shortening related to the Feleches thrust and associated folds. The top of the Lower–Middle Devonian limestones was used as a reference surface in cross-sections IV–IV′ and VI–VI′ (Fig. 13a and c), and it has been assumed that this stratigraphic unit can be fairly accurately restored using the bed-length method. Because the Feleches thrust is deformed by the Sobia imbricate system, a regional datum has been established to remove the effect of late structures (Fig. 13c). The shortening estimated is similar in both cases (4.82 km in the case of the thrust and 4.59 km in the case of the folds; Fig. 13b and d), which supports the hypothesis of lateral evolution of the Feleches thrust into folds. In this particular case, folds located to the S accommodate the displacement due to thrusting to the N.

4. Kinematic evolution of the large-scale fault-propagation folds

The overprinting relationships between the structures have allowed us to establish the structural history of the area. Both major imbricate thrust systems (the Sobia system and the Pedroveya system) deform E-directed thrusts and their related folds. In some cases, these old thrusts and folds are simply transported along the imbricate thrust systems (e.g. the thrusts located below the folded Lower–Middle Devonian limestone in cross-section IV–IV′ in Fig. 6). In other cases they are also folded and offset (cross-sections I–I′, II–II′, III–III′ and VII–VII′ in Figs. 3–5 and 9, respectively). The old thrusts caused obliquities between beds, thickness variations, and increased the number of discontinuities and weak surfaces (e.g. thrust surfaces) before major folding. Therefore, the old structures must have influenced the kinematic evolution and final geometry of the major folds.

The backlimb of the major antiforms thickened during the initial stages of amplification of the major fault-propagation folds. This was caused by propagation of imbricate thrusts that partially reactivated previous thrusts (cross-section II–II′ in Fig. 4), and formation of related folds that repeated the stratigraphic sequence. These structures developed mainly during the initial amplification stages because: (1) the geometrical relationships between bedding and thrusts indicate that they deformed gently dipping stratigraphic sequences, (2) they affect mainly the lower rocks of the Paleozoic sequence (i.e. thrusts and deformation in general propagate upwards), and (3) some of the thrusts are deformed by the major folds (e.g. the imbricate thrusts of the Sobia system within the backlimb of the Caranga–Trubia antiform in cross-section II–II′ in Fig. 4). During the last stages of fold amplification, the forelimb of the major antiforms thinned due to imbricate breakthrough thrusts, and thickened locally due to development of some thrust-related folds (Figs. 2–9). We believe that these imbricate breakthrough thrusts developed during the final amplification stages because: (1) the geometrical relationships between bedding and thrusts indicate that they offset previously steepened beds, and (2) they are mainly located in the upper half of the Paleozoic sequence. Summarizing, once folding initiated, thrust faults started to propagate, and continued propagating resulting in the transportation of the major folds. During amplification of the major folds, local thickening occurred as some imbricate thrusts propagated through incompetent stratigraphic units. This is particularly evident in the hinge zone of the antiforms, where a number of mesoscopic folds developed within ductile materials with thin intercalations of competent rocks (e.g. the folds in both major antiforms in Figs. 3–9, when cored by Lower Devonian rocks).

Fold amplification ceased when the folds acquired steep to overturned limbs and axial surfaces, in some cases facing opposite to the tectonic transport direction. This disposition is interpreted to be the result of the back-rotation of the folds due to emplacement of thrusts during major folding, and transportation over younger thrust ramps located towards the foreland.

5. Fold/thrust transitions

5.1. Transition at regional scale

At regional scale, a zone to the S of the study area deformed mainly by thrust transitions to a zone that comprises the study area and farther N where large-scale folds predominate (e.g. Soler, 1967; Pello, 1972; Julivert and Arboleya, 1984; Alonso et al., 1991; Alonso and Marcos, 1992). The S–N transition from an area where fractures (thrusts) and related fault-bend folds predominate into the study area where thrust-tip folds are most evident should reveal variations in the parameters that influence the deformation mechanisms. The most critical factors that control the widely varying fold/thrust styles include:

presence and geometry of old structures, depth of burial, strain rate, amount of shortening, and relative thicknesses and competences of the sedimentary pile (i.e. mechanical stratigraphy; Jamison, 1992; Rowan and Kligfield, 1992). The combination of such elements determines the response to regional compression through faulting, folding and penetrative strain.

No pre-Variscan structures within the Paleozoic sequence have been documented in the Cantabrian Zone, so that the Variscan deformation event affected a nearly layer-cake stratigraphy. The subsurface structure of the study area (as illustrated in the cross-sections; Figs. 3–9), which assumes the occurrence of a basal detachment from which the thrusts emanate, located at the same depth as in regions S of the study area (see interpretations of regional seismic profiles by Pérez-Estáun et al. (1994, 1995)). The Paleozoic succession, especially the Devonian sequence, shows facies and thickness changes in an E–W direction within the study area (e.g. Bulnes, 1995; Bulnes and Marcos, 2001). Nevertheless, this succession shows no significant variations in the N–S direction within the study area and further to the S, suggesting similar mechanical behavior in this direction as well. Moreover, small-scale fault-bend, fault-propagation, detachment folds and folds not related to thrusts affect the same stratigraphic units within the study area. This suggests that the mechanical features of the rocks do not substantially influence the type of fold developed. The shortening accommodated by the structures that appear in the study area is relatively constant irrespective of lateral variations in structural style (type, number, size of the structures, etc.; Bulnes, 1995; Bulnes and Marcos, 2001). Therefore, the occurrence of inherited structures, the stratigraphy, and the amount of shortening are not responsible for the S–N change in structural style.

5.2. Transition within the study area

The geological map and sections across the study area show that the transition from folds to thrusts not only occurs with major structures, but also at smaller scales (Figs. 2–9). In many cases, the transition from folds to thrusts reflects changes in structural style up-section. Slip is dissipated up-section mainly by folding. In some sectors, however, the change in structural style occurs not only up-section, but also along strike. For instance, in the central part of the study area, the Xanas thrust exhibits a hanging wall anticline cored by Lower–Middle Devonian rocks to the W of the Pedroveya village (cross-section IV–IV′ in Fig. 6), whereas to the N Carboniferous limestones are subparallel to the thrust surface (cross-section V–V′ in Fig. 7). In the same sector, the Alfilorios thrust shows a change in structural style along strike. To the SW of the Soto de Ribera village, this thrust offsets the forelimb of a hanging wall anticline cored by Middle Devonian rocks (cross-section VI–VI′ in Fig. 8), whereas to the S the thrust does not cut a hanging wall anticline cored by Lower–Middle Devonian rocks (cross-sections IV–IV′ and V–V′ in Figs. 6 and 7, respectively). In these particular cases, shortening in the upper levels is accommodated by folding and thrusting to the N, whereas it is consumed by folding southwards. The Feleches thrust also exhibits variations in structural style along strike (cross-sections VI–VI′ and VII–VII′ in Figs. 8 and 9, respectively). In the northern part of the study area, this thrust displays a large hanging wall flat at the base of the Lower–Middle Devonian limestones, whereas to the S the thrust surface disappears and these rocks are deformed by a number of well-developed folds and subvertical faults (Figs. 2a, 6, 8 and 9).

The observations above show that vertical/lateral transitions from thrusts into folds occur at small scale in the study area. At large scale, the Sobia thrust becomes the Caranga–Trubia antiform and the Proaza–Las Caldas synform to the N. This transition is due to the N plunge of most folds in the western part of the study area, except for a small sector in the central part (Fig. 10). However, fold/thrust transitions also occur in the opposite sense. For instance, the Pedroveya imbricate thrust system evolves into the Pedroveya antiform and Mostayal synform to the S. This is due to the dominant S plunge of the folds in the easternmost part of the study area (Fig. 10).

6. Comparison between the large-scale fault-propagation folds and theoretical models

The complex internal structure of the large-scale fault-propagation folds results from the development of thrusts and related folds before, during, and after their formation. Therefore, comparison with theoretical models of fault-propagation folds that relate the fold geometry to the ramp dip (e.g. Jamison, 1987; Chester and Chester, 1990; Mitra, 1990; Suppe and Medwedeff, 1990) is difficult. However, some of the structural features displayed by the studied folds permit a qualitative comparison.

6.1. Dip of the limbs and axial surfaces

In general, the studied folds have small interlimb angles and the dip of the limbs is steep to overturned. In some areas the axial surfaces dip steeply in the opposite direction to the thrust ramp, so that the fold asymmetry is reversed and the folds face opposite to the tectonic transport direction. This particular disposition of the limbs and axial surfaces is observed in some theoretical models of fault-propagation folds. According to many classical models of fault-propagation folds (Jamison, 1987; Suppe and Medwedeff, 1990; Mosar and Suppe, 1992), steep limbs and axial surfaces, sometimes overturned, require high dips of the thrust ramp coupled with large amounts of forelimb thinning. However, the anticline backlimb is parallel to the thrust ramp and their dips do not exceed 60°. The hybrid fault-propagation/detachment fold model proposed by Chester and Chester (1990) and Marret and Bentham (1997) predicts

that steep limbs and axial surfaces of anticlines can be obtained with shallow dips of the thrust ramps irrespective of thickness variations. In the case where the fold limbs reach dips of 90°, the folds become detachment structures, so that the thrusts do not exhibit significant ramps. These observations suggest that the present-day disposition of the natural folds analyzed did not result from simple fault-propagation folding theory. According to Mitra (1986), the dip towards the foreland of the limbs and axial surfaces of fault-propagation folds may result from transportation of the folds over younger thrust ramps located to the foreland. Alternatively, Al Saffar (1993) proposed a model in which the formation of several generations of fault-propagation folds due to imbricate thrusting forced the limbs and axial surfaces to dip towards the foreland. To first order both theoretical models (Mitra, 1986; Al Saffar, 1993) are partially consistent with the interpretation proposed in this paper. For instance, in cross-sections I–I′, III–III′, IV–IV′, V–V′ and VI–VI′ (Figs. 3 and 5–8, respectively), the elevation and passive rotation of the Caranga–Trubia antiform may be due to the displacement along the easternmost thrusts of the Sobia imbricate thrust system, which is consistent with the Mitra (1986) model. In addition, the geometry of the Pedroveya antiform in the area located to the S of the Pedroveya village (Fig. 12) can be partially explained according to the Al Saffar (1993) model. Thus, the development of minor fault-propagation folds related to the successive emplacement of thrusts of the Pedroveya imbricate thrust system contributed to the overturned disposition of the beds within the backlimb of the antiform and to the E dip of its axial surface.

6.2. Thickness variations

The natural large-scale folds analyzed in this paper show many minor structures that accommodated shortening in upper structural levels and that caused forelimb thinning and backlimb thickening. According to our observations, backlimb thickening occurred mainly during the initial fold amplification stages, whereas forelimb thinning took place mainly during the latest amplification stages. Many theoretical models for fault-propagation folds allow for changes in bed thickness (Jamison, 1987; Chester and Chester, 1990; Mitra, 1990; Suppe and Medwedeff, 1990; Erslev, 1991; Mosar and Suppe, 1992; Al Saffar, 1993; Hardy and Ford, 1997; Marret and Bentham, 1997; Allmendinger, 1998). However, with the exception of Mitra (1990), these models only account for forelimb thickness variations. Mitra (1990) proposed a kinematic model in which the interlimb angle of the fold decreases with fault propagation due to forelimb rotation. Layer thickening occurs in the initial stages, which can be distributed throughout the fold or localized by thrusting. At some stage, the fold is too tight for efficient migration of the hinge. The anticline then becomes locked and the steep forelimb undergoes thinning because it is oriented at a high angle to the principal regional compressive stress. The structures that we observed in the antiforms agree broadly with those modeled by Mitra (1990). If correct, the forelimbs of the antiforms that we analyzed were amplified by a combination of limb rotation and hinge migration.

6.3. Imbricate thrust system

The natural fault-propagation folds in this study involve imbricate thrusts that cut parts of the folds. Some theoretical models proposed to date address breakthrough structures derived from initial fault-propagation folds (e.g. Jamison, 1987; Mitra, 1990; Suppe and Medwedeff, 1990; Al Saffar, 1993; Mercier et al., 1997). Many of these models consist of fault-propagation folds related to a single thrust. However, in the study area the thrust associated with the folds is not a single fault, but an imbricate thrust system. All theoretical models show thrusts that propagate through the axial surface of the fault-propagation anticline, the forelimb, and/or the frontal syncline. In the study area, most of the imbricate thrusts break through the forelimbs, and some through the axial surfaces of the antiforms and synforms. However, unlike the theoretical models, there are also imbricate thrusts that break through the backlimb of the antiforms (e.g. see sketch of cross-section II–II′ in Fig. 4). In the study area, breakthrough faults consist mainly of imbricate thrust ramps that, unlike many theoretical models, have cross-sectional listric shapes. According to Mitra (1990) and Al Saffar (1993), thrust ramps within imbricate thrusts may form by progressive abandonment of slip on deeper thrusts. In all the models, except for Al Saffar (1993), folding stops before the thrusts break through the structures. However, the imbricate thrusts that belong to the Sobia system and break through the backlimb of the Caranga–Trubia antiform are partially folded by the antiform (cross-section II–II′ in Fig. 4), which suggests they are coeval to major folding. Al Saffar (1993) presented a model of fault-propagation folds in which several generations of fault-propagation folds form. These folds nucleate in the core of folds formed in a previous generation. In the natural folds presented here, there are minor folds (mainly fault-propagation folds) related to some of the thrusts that break through the major folds. However, they nucleate in both the core and the limbs of the major folds. Therefore, the natural examples presented here do not precisely match any of the theoretical models of fault-propagation folds involving breakthrough structures and/or several generations of fault-propagation folding. They may be interpreted as a complex combination of several models.

7. Discussion and conclusions

The geometry of the structures observed in the study area and the structural overprinting criteria indicate that folding and thrusting are kinematically-linked processes. Thus, the kilometer-scale folds that outcrop in the study area are

interpreted as fault-propagation folds. From a regional point of view, we conclude that in the northwestern part of the Cantabrian Zone, the transition from a region to the S where well-developed thrusts and related fault-bend folds dominate into an area to the N where folds are the most conspicuous structures, takes place by fault-propagation folding. This conclusion might be of interest in understanding regional lateral changes in structural styles in other foreland fold-thrust belts.

The internal geometry of the major fault-propagation folds is complex due to motion of thrusts and formation of related folds at different stages during deformation. Although the major deformation mechanism was fault-propagation folding, several mesoscopic-scale deformation mechanisms accommodated shortening. Bedding-subparallel thrusting directed towards the foreland and related folding occurred while beds were still subhorizontal or gently dipping. These thrusts, together with the ones that developed in the backlimb of the antiforms during the initial stages of major folding, thickened this limb. Subsequently, bedding was substantially steepened, especially in the forelimbs of the major folds, which were extended due to later thrusting. Eventually, the beds and structures involved in the major folds underwent back-rotation due to stacking of imbricate thrust systems within the major folds and translation over hinterland-dipping thrust ramps located towards the foreland.

The complex internal structure shown by the major folds together with significant variations in structural style up-section and along strike, result in natural examples of fault-propagation folds with an atypical three-dimensional geometry. The vertical evolution can be observed mainly due to the plunge of the structures. In general, well-developed thrusts occur mainly in the lower part of the succession, whereas folds, in most cases cut by thrusts, appear in the upper part of the succession. The up-section evolution of the fault-propagation folds can be observed on the map in N–S direction.

We would like to emphasize the differences in the fold geometry and kinematics documented here versus the theoretical fault-related fold models published. Despite the fact that the field examples studied are considerably more complex than the kinematic models of fault-propagation folds proposed to date, a qualitative comparison has been carried out between the natural examples and models in terms of: (1) beds and axial surfaces dipping towards the foreland, (2) thickness variations, (3) thrusts that break through the structures, and (4) formation of various generations of fault-propagation folds. The main reason to compare them is that in the natural examples only the final state is known, whereas in the theoretical models the structural history can be interpreted. In spite of the significant differences between the field examples and the theoretical models, their comparison can ultimately provide useful information for a better understanding of fold/thrust interaction.

Geometrical techniques are commonly employed to predict the geometry of the folds/thrusts at depth in areas where no subsurface data are available. These techniques use field information such as dips and thickness of the exposed beds. Many of these graphical/numerical techniques assume that the thickness variations are distributed homogeneously through the fold limbs for simplicity, and that the limbs maintain approximately constant dips. However, the natural examples studied show that heterogeneous thickness and dip changes can be common in some upper crustal domains subject to tight folding. Small-scale folds, imbricate thrusts, and similar structures play a dominant role in thickening/thinning the fold limbs and hinges. As a consequence, local dip and thickness measurements in these areas should not be used to predict the geometry of the structures at depth. Only accurate field mapping over a reasonably large area allows integration of enough field measurements and permits a reliable extrapolation of the geometry of the structures at depth.

The crests of major anticlines, backlimb thrusts, imbricate thrusts in the forelimbs and overturned beds in footwall synclines are very important structural hydrocarbon traps in fold-and-thrust belts (Mitra, 1990). The results presented in this paper suggest that both limbs and hinges of large-scale fault-propagation folds with small interlimb angles may be intensely fractured, and therefore, they may be excellent fractured reservoir targets. However, the internal structure of these folds appears to vary significantly along strike (size, number and geometry of the small-scale structures), which makes it difficult to extrapolate the lateral geometry and continuity of the traps.

Acknowledgements

M. Bulnes acknowledges financial support by a fellowship (1988–92) within the Formación del Personal Investigador (F.P.I.) program funded by the Ministerio de Educación y Ciencia. We are grateful to projects AMB98-1012-CO2-02 (Actividad sismotectónica, estructura litosférica y modelos de deformación varisca y alpina en el NO de la Península Ibérica) and PB98-1557 (Mecanismos de plegamiento: teoría y aplicaciones en geología económica y regional) funded by the Ministerio de Educación y Cultura, and to Acción Integrada Hispano-Británica HB 1999-0038 (Cinemática de pliegues y estructuras menores asociadas a cabalgamientos a partir del estudio de materiales sintectónicos y de su modelización) funded by the Ministerio de Educación y Cultura and the British Council. We would like to thank Ted Apotria, Shankar Mitra and Richard R. Gottschalk for their constructive reviews. Special thanks to Alberto Marcos, Juan Luis Alonso, Joaquina Alvarez-Marrón and Andrés Pérez-Estaún for their contributions to this study. We thank Josep Poblet for helping us to improve the English.

References

Allmendinger, R.W., 1998. Inverse and forward numerical modeling of trishear fault-propagation folds. Tectonics 17, 640–656.

Alonso, J.L., Marcos, A., 1992. Nuevos datos sobre la estratigrafía y la estructura de la sierra del Pedrosu (Zona Cantábrica, NW de España): implicaciones tectónicas. Revista de la Sociedad Geológica de España 5, 81–88.

Alonso, J.L., Aller, J., Bastida, F., Marcos, A., Marquínez, J., Pérez-Estaún, A., Pulgar, J., 1991. Mapa Geológico de España E. 1:200.000, Hoja no. 2 (3–1), Avilés. Instituto Tecnológico y Geominero de España.

Al Saffar, M., 1993. Geometry of fault-propagation folds: method and application. Tectonophysics 223, 363–380.

Bulnes, M., 1989. La estructura del área situada en el entorno de las localidades de Trubia, Proaza y Sama de Grado (Zona Cantábrica, NO de España). MSc. thesis, Universidad de Oviedo.

Bulnes, M., 1991. Geometry and Structural Evolution of the Caranga Antiformal Stack (Cantabrian Zone, NW Spain). Abstracts. The Geometry of Naturally Deformed Rocks. Mitt. Aus den Geol. Inst. ETH Zürich, Neue Folge, p. 107.

Bulnes, M., 1992. Geometría y evolución estructural del antiforme de Caranga. Actas de las sesiones Científicas. III Congreso Geológico de España 1, 274–278.

Bulnes, M., 1995. La estructura geológica del valle del Río Trubia (Zona Cantábrica, NO de España). Ph.D. thesis, Universidad de Oviedo.

Bulnes, M., 1999. Progressive thrust/fold development within large-scale fault-propagation folds of Variscan age (Cantabrian Zone, NW Iberian Peninsula). Program with Abstracts, Thrust Tectonics 99, University of London, pp. 146–149.

Bulnes, M., Marcos, A., 2001. Internal structure and kinematics of Variscan thrust sheets in the valley of the Trubia River (Cantabrian Zone, NW Spain): regional tectonic implications. International Journal of Earth Sciences 90, 287–303.

Chamberlin, R.T., 1910. The Appalachian folds of central Pennsylvania. Journal of Geology 18, 228–251.

Chester, J.S., Chester, F.M., 1990. Fault-propagation folds above thrusts with constant dip. Journal of Structural Geology 12, 903–910.

Erslev, E.A., 1991. Trishear fault-propagation folding. Geology 19, 617–620.

Gallastegui, J., Pulgar, J.A., Alvarez-Marrón, J., 1997. 2D seismic modeling of the Variscan foreland thrust and fold belt crust in NW Spain from ESCIN-1 deep seismic reflection data. Tectonophysics 269, 21–32.

García Fuente, S., 1952. Geología del Concejo de Teverga (Asturias). Boletín del Instituto Geológico y Minero de España LIXV, 345–456.

García Fuente, S., 1959. Mapa Geológico de España. Esc. 1:50.000, Hoja no. 77 (La Plaza, Teverga). Instituto Geológico y Minero de España, Madrid.

Hardy, S., Ford, M., 1997. Numerical modeling of trishear fault propagation folding. Tectonics 16, 841–854.

Jamison, W.R., 1987. Geometric analysis of fold development in overthrust terranes. Journal of Structural Geology 9, 207–219.

Jamison, W.R., 1992. Stress controls of fold thrust style. In: McClay, K.R. (Ed.). Thrust Tectonics. Chapman and Hall, London, pp. 155–164.

Julivert, M., Arboleya, M.L., 1984. A geometrical and kinematical approach to the nappe structure in an arcuate fold belt: the Cantabrian nappes (Hercynian chain, NW Spain). Journal of Structural Geology 6, 499–519.

Marcos, A., 1968. La tectónica de la Unidad de La Sobia-Bodón. Trabajos de Geología, Universidad de Oviedo 2, 59–87.

Marcos, A., Pérez-Estaún, A., Pulgar, J.A., Aller, J., García-Alcalde, J.L., Sánchez de Posada, L.C., 1980. Mapa Geológico de España. Esc. 1:50.000, Hoja no. 77 (La Plaza). Instituto Geológico y Minero de España, Madrid.

Marret, R., Bentham, P.A., 1997. Geometric analysis of hybrid fault-propagation/detachment folds. Journal of Structural Geology 19, 243–248.

Mercier, E., Outtani, F., Frizon de Lamotte, D., 1997. Late-stage evolution of fault-propagation folds: principles and example. Journal of Structural Geology 19, 185–193.

Mitra, S., 1986. Duplex structures and imbricate thrust systems: geometry, structural position and hydrocarbon potential. American Association of Petroleum Geologists Bulletin 70, 1087–1112.

Mitra, S., 1990. Fault-propagation folds: geometry, kinematics and hydrocarbon traps. American Association of Petroleum Geologists Bulletin 74, 921–945.

Mosar, J., Suppe, J., 1992. Role of shear in fault-propagation folding. In: McClay, K.R. (Ed.). Thrust Tectonics. Chapman and Hall, London, pp. 123–132.

Pello, J., 1972. Geología de la región central de Asturias. Ph.D. thesis, Universidad de Oviedo.

Pérez-Estaún, A., Bastida, F., Alonso, J.L., Marquínez, J., Aller, J., Alvarez Marrón, J., Marcos, A., Pulgar, J.A., 1988. A thin-skinned tectonics model for an arcuate fold and thrust belt: the Cantabrian Zone (Variscan Ibero–Armorican Arc). Tectonics 7, 517–537.

Pérez-Estaún, A., Pulgar, J.A., Banda, E., Alvarez-Marrón, J., ESCI-N Research Group (Marcos, A., Bastida, F., Alonso, J.L., Aller, J. Farias, P., Martínez-Catalán, J.R., Comas, M.C., Dañobeitia, J.J., Córdoba, D.), 1994. Crustal structure of the External Variscides in NW Spain from deep seismic reflection profiling. Tectonophysics 232, 91–118.

Pérez-Estaún, A., Pulgar, J.A., Alvarez-Marrón, J., ESCI-N Group (Marcos, A., Bastida, F., Aller, J., Marquínez, J., Farias, P., Alonso, J.L., Gutiérrez, G., Gallastegui, J., Rodríguez Fernández L.R., Heredia, N., Bulnes, M., Banda, E., Martínez-Catalán, J.R., Córdoba, D, Dañobeitia, J.J., Comas, M.C.), 1995. Crustal structure of the Cantabrian Zone: seismic image of a Variscan foreland thrust and fold belt (NW Spain). Revista de la Sociedad Geológica de España 8, 307–319.

Rowan, M.G., Kligfield, R., 1992. Kinematics of large-scale asymmetric buckle folds in overthrust shear: an example from the Helvetic nappes. In: McClay, K. (Ed.). Thrust Tectonics. Chapman and Hall, London, pp. 165–173.

Soler, M., 1967. Evolución longitudinal del cabalgamiento de Peña Sobia (Asturias). Acta Geológica Hispánica 2, 82–84.

Suppe, J., 1985. Principles of Structural Geology. Prentice Hall, New Jersey.

Suppe, J., Medwedeff, D.A., 1990. Geometry and kinematics of fault-propagation folding. Eclogae Geologicae Helvetiae 83, 409–454.